

# Using Ultrasonic and Infrared Sensors for Distance Measurement

Tarek Mohammad

**Abstract**—The amplitude response of infrared (IR) sensors depends on the reflectance properties of the target. Therefore, in order to use IR sensor for measuring distances accurately, prior knowledge of the surface must be known. This paper describes the Phong Illumination Model for determining the properties of a surface and subsequently calculating the distance to the surface. The angular position of the IR sensor is computed as normal to the surface for simplifying the calculation. Ultrasonic (US) sensor can provide the initial information on distance to obtain the parameters for this method. In addition, the experimental results obtained by using LabView are discussed. More care should be taken when placing the objects from the sensors during acquiring data since the small change in angle could show very different distance than the actual one. Since stereo camera vision systems do not perform well under some environmental conditions such as plain wall, glass surfaces, or poor lighting conditions, the IR and US sensors can be used additionally to improve the overall vision systems of mobile robots.

**Keywords**—Distance Measurement, Infrared sensor, Surface properties, Ultrasonic sensor.

## I. INTRODUCTION

INFRARED (IR) sensors are extensively used for measuring distances. Therefore, they can be used in robotics for obstacle avoidance. They are cheaper in cost and faster in response time than ultrasonic (US) sensors. However, they have non-linear characteristics and they depend on the reflectance properties of the object surfaces. So knowledge of the surface properties must be known prior. In other words, the nature in which a surface scatters, reflects, and absorbs infrared energy is needed to interpret the sensor output as distance measure [1]. IR sensors using reflected light intensity to estimate the distance from an object are reported in the bibliography [4-6]. Their inherently fast response is attractive for enhancing the real-time response of a mobile robot [2]. Some IR sensors described in the bibliography are based on the measurement of the phase shift, and offer medium resolution from 5 cm to 10 m [7], but these are very expensive.

Ultrasonic (US) sensors are also widely used to measure distances. Thus they have provided a reliable source of obstacle detections. Since they are not vision-based, they are useful under conditions of poor lighting and transparent objects. However, US sensors have limitations due to their wide beam-width, sensitivity to specular surfaces [8], and the inability to discern objects within 0.5 m [7]. Because of the typical specular nature of the US waves reflection, only reflecting objects that are almost normal to the sensor acoustic axis may be accurately detected [3]. The US sensors described

in [7, 10] have precision of less than 1 cm in distance measurements of up to 6m. However, the time of flight (ToF) measurement is the most accurate method among the measurements used. This ToF is the time elapsed between the emission and subsequent collection of a US pulse train traveling at the speed of sound, which is approximately 340 m/s, after reflection from an object. For single measurement, this causes large response time, for example, 35 ms for objects placed 6m away. In addition, they offer poor angular resolution.

In an unknown environment, it is important to know about the nature of surface properties in order to interpret IR sensor output as a distance measurement. Here, US sensor can play an important role in determining the surface properties. The co-operation between the US and IR sensors are utilized to create a complementary system that is able to give reliable distance measurement [1]. They can be used together where the advantages of one compensate for the disadvantages of the other. The integration of the information supplied by the multiple US and IR sensors can be a means to cope with the spatial uncertainty of unknown, unstructured environments in several applications of advanced robotics, such as flexible industrial automation, service robotics, and autonomous mobility [3].

This paper details a method that determines the infrared reflectance properties of a surface and then calculates the distance by using these properties. The basis of our approach is the Phong Illumination Model [10], which is usually used in computer graphics routines [1]. This model is able to figure out the reflectance properties of any surface illuminated by a point light source such as IR LED. However, this method requires other sensing modalities to get the information on the distance to obstacle initially. US sensors can fulfill the requirements in unknown environment. Then we tested and characterized the effects of distance on two sensors. National Instruments Data Acquisition System with LabView software was used to collect data due to its ability to measure the smallest possible increments of voltage drop/rise.

## II. DESCRIPTION OF SENSORS

Our approach to the use of sensors for measuring distances is based on the ideology that the use of expensive transducers and complex signal processing techniques should be avoided if we want a better cost-performance ratio compared to that of more sophisticated imaging systems, such as the ones based on stereopsis or laser scanning. One of the most attractive advantages of using LED, Phototransistors, Ultrasonic sensor, and IR LED sensor lies in their low cost and relative simplicity of use.

### A. LED, Fiber Optic cables and Phototransistor

We designed and built a sensor system by using a LED, two fiber optic cables and a phototransistor as shown in Fig. 1. One part of the circuit was designed using a variable resistor along with the fiber optic red LED (IF-E96). The positive end of the IF-E96 was connected to 5VDC from the DC power supply. Before being grounded, the negative end was connected to a resistor. By changing the value of resistance of the variable resistor, the intensity of light can be varied. The other part of the circuit was designed using a 1  $\mu$ F capacitor, a resistor and a variable resistor with the phototransistor (IF-D92). The positive end was connected to 5 VDC from the power supply. The negative end of the IF-D92 was connected to the ground terminal.

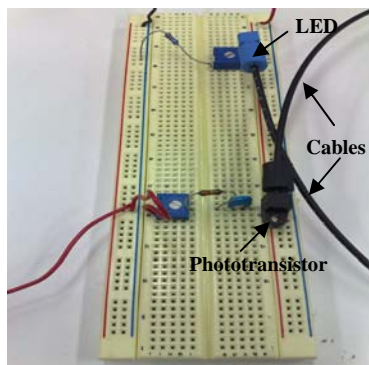


Fig. 1 Sensor made of a LED, two fiber optic cables and a phototransistor

The function of the phototransistor is to detect the energy reflected by an obstacle from the LED. However, it was unable to detect any reflected energy for distances more than 20 cm. Moreover, obtaining suitable alignment of two fiber optic cables and angle of incidence of the light were very difficult. Therefore, we can conclude that this is a worse sensing system for measuring considerable distance accurately.

### B. Ultrasonic Sensor Properties

The ultrasonic sensor used for this paper is UB400-12GM-U-V1 which has 12 mm cylindrical housings. It generates frequency sound waves of 310 kHz and evaluates the echo which is received back. It has sensing range of 50 – 400 mm with unusable range of 0 – 50 mm and less than 50 ms response time. Sensor can calculate the time interval between sending the signal and receiving the echo to determine the distance to an object. In this experiment, we used the change in US sensor readings to obtain the information on distances to obstacle. By taking multiple readings to various distances, we found that the US sensor could produce a fairly accurate representation of the object location. However, it faced difficulty with round-shaped objects.

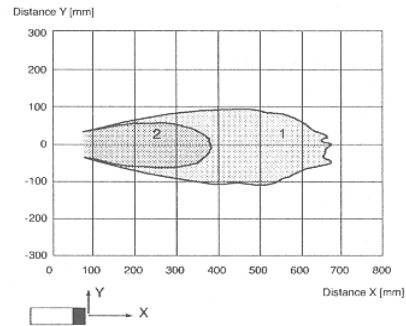


Fig. 2 Target Response Curves of US sensor Curve 1 for flat surface 100 mm  $\times$  100 mm Curve 2 for round bar, R 25 mm

### C. Infrared Sensor Properties

Experiments for the measuring distances were carried out using an infrared sensor consisted of one infrared LED and a pair of silicon phototransistors. The functions of the phototransistors are to detect the energy reflected by an obstacle from the LED. As a result the signal returned from the sensor is dependant on the energy emitted from the LED and the detectable range of the photo-transistors. These limitations caused problems at the upper and lower end of the sensor range. When the sensor was positioned close to an obstacle, within 3 cm and aimed about 90° from the surface of an obstacle, the photo-transistors began to saturate, and was unable to detect any additional reflected energy. On the other hand, readings taken above 45 cm were indistinguishable due to the lack of energy detected by the phototransistors. Nevertheless, within this range the sensors behaved monotonically with respect to distance. Thus, within the range of an infrared sensor, it is possible to utilize the signal for distance estimation.

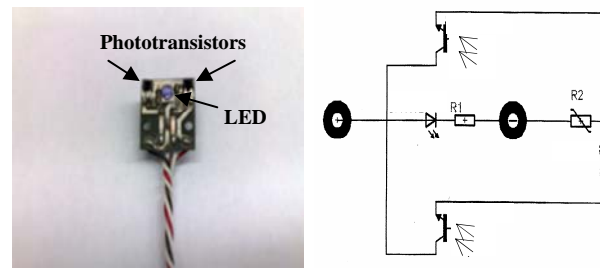


Fig. 3 IR sensor and its circuit

## III. METHODOLOGY

The process of measuring distance to an obstacle by using IR sensors can be divided into three steps. First, the properties of the surface of the obstacle are determined. Secondly, the angle or orientation of the surface relative to the sensor is determined. Finally, the distance is calculated by using the information obtained in first two steps.

### A. Determination of Surface Properties

As light energy hits a surface, some portion of it scattered or absorbed and rest of the energy is reflected. Different surfaces scatter, absorb and reflect light in different portions.

It is obvious that black surface will absorb more light than a white surface, and a shiny smooth surface will reflect more energy than a rough surface. The Phong Model can provide a simplified description of these effects into four constants:  $C_0$ ,  $C_1$ ,  $C_2$ , and  $n$ . The Phong equation for intensity of energy,  $I$ , reflected from a surface is

$$I = C_0 (\vec{\mu}_s \cdot \vec{\mu}_n) + C_1 (\vec{\mu}_r \cdot \vec{\mu}_v)^n + C_2 \quad (1)$$

where,  $\vec{\mu}_s$ ,  $\vec{\mu}_n$ ,  $\vec{\mu}_r$ , and  $\vec{\mu}_v$  are the light source, surface normal, reflected, and viewing vector, respectively, as shown in Fig. 4.

A sensor emitting infrared energy and the interaction of the energy with a flat surface is shown in Fig. 5. When comparing Fig. 4 with Fig. 5, one can determine of the value of  $(\vec{\mu}_s \cdot \vec{\mu}_n)$  and  $(\vec{\mu}_r \cdot \vec{\mu}_v)$ . The angle between the source vector and the normal vector of the surface is  $\alpha$ . Also, if one assumes that the emitter and receiver are in the same position, then the angle between the viewing vector and the reflected vector is  $2\alpha$ . Therefore, Equation (1) becomes:

$$I = C_0 \cos(\alpha) + C_1 \cos^n(2\alpha) + C_2 \quad (2)$$

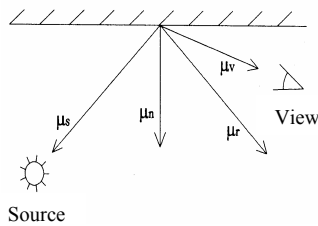


Fig. 4 Phong Model

Again, the energy absorbed by the phototransistors is a function of Intensity ( $I$ ), distance traveled ( $2\ell$ ), and the area ( $A$ ) of the sensor.

$$E = \frac{IA}{(2\ell)^2} \quad (3)$$

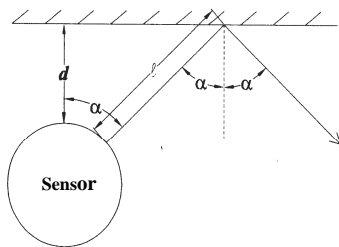


Fig. 5 Emission and Reflection of an infrared signal by sensor

From Fig. 5,  $\ell$  can be expressed in terms of  $d$ ,  $\alpha$ , and the radius of the sensor ( $r$ ).

$$\ell = \frac{d}{\cos(\alpha)} + r \left( \frac{1}{\cos(\alpha)} - 1 \right) \quad (4)$$

By combining (2), (3), (4) with the assumption that  $C_2 = 0$ ,  $n = 1$  and  $A$  is constant, the energy absorbed by the sensor can be expressed as

$$E = \frac{C_0 \cos(\alpha) + C_1 \cos(2\alpha)}{\left[ \frac{d}{\cos(\alpha)} + r \left( \frac{1}{\cos(\alpha)} - 1 \right) \right]^2} \quad (5)$$

Finally,  $C_0$  and  $C_1$  in (5) indicate the infrared characteristics of an obstacle. One can determine these values by taking infrared readings at known distances ( $d$ ), and angles ( $\alpha$ ). Once  $C_0$  and  $C_1$  are known,  $E$  can be obtained for a given angle and distance by using (5).

#### B. Determination of the Angle of a Surface

The relative angle of the sensor to the surface must be determined to simplify the calculating the surface properties and the distance of an obstacle. The maximum reading of the sensor will occur at  $\alpha = 0$ . In Fig. 6, the spike occurs where the direction of the IR signal corresponds to the surface normal ( $\alpha = 0$ ).

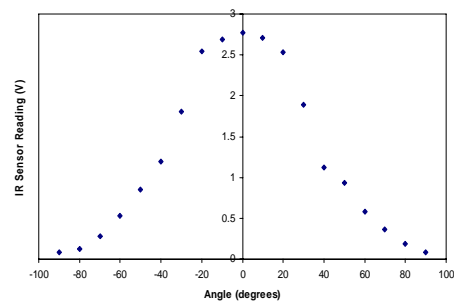


Fig. 6 Data collected from a flat surface 10 cm from sensor at different angles

#### C. Calculating the Distance to an Object

After obtaining the properties of a surface and the relative angle of the surface, it becomes easier to calculate the distance. From (5), the distance ( $d$ ) can be expressed as:

$$d = r(\cos(\alpha) - 1) + \cos(\alpha) \sqrt{\frac{C_0 \cos(\alpha) + C_1 \cos(2\alpha)}{E}} \quad (6)$$

Thus the infrared readings can be interpreted to distance between the obstacle and the sensor.

### IV. RESULTS AND DISCUSSION

Before using LabView, we need to calibrate both of the sensors. These allow us to obtain formula for each sensor which we could use while creating VI. During calibration, we used different surfaces and selected the one which provided the best readings.

### A. Calibration of US Sensor

From the results of the calibration of US sensor, we observed that:

The amplitude from the US sensor is dependent on the distance and orientation of the obstacle relative to the sensor. The output signal from the US sensor does not depend on surface color and smoothness. The Fig. 7 shows the US sensor has almost linear characteristic within its usable range.

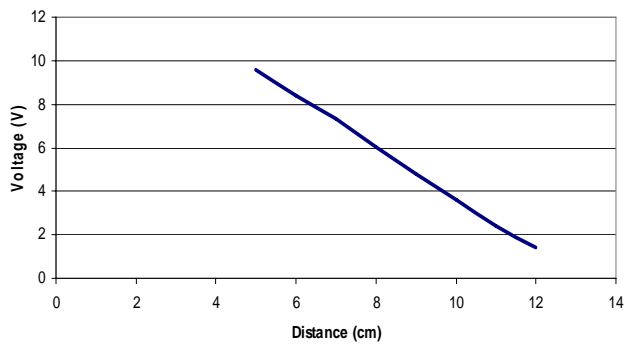


Fig. 7 Calibration curve for a single US sensor

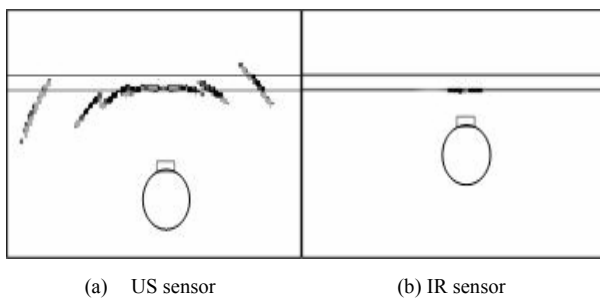


Fig. 8 Distance data from the flat surface

### B. Calibration of IR Sensor

For calibrating the IR sensor, we used different objects with different color and surface smoothness. They were silver finished metal block with smooth surface, white plastic board, unfinished wood, and black notebook with rough surface. The calibration curve for the IR sensor is shown in Fig. 9.

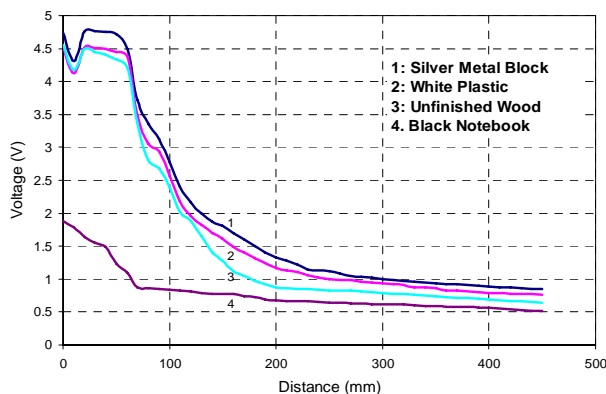


Fig. 9 Calibration curve for a single IR sensor

From the results of the calibration, we found that:

The amplitude from the IR sensor is dependent on the reflectivity of the obstacle as expected. The amplitude from the IR sensor is slightly dependent on the environmental conditions such as sunlight, artificial lights, unless the external source is directly pointed towards the sensor. For angles within 10-20°, the orientation of the reflecting surface does not have much effect on the IR sensor amplitude. From Fig. 9, it is evident that the IR sensor has non-linear characteristic.

### C. Experimental Setup

LabView software of National Instruments with DAQ (data acquisition board), SCB-68 shielded I/O block connector, Tektronix 2-channel digital oscilloscope were used to carry out the experiment. The US sensor was connected to 25 VDC and the IR sensor was connected to 5 VDC from the BK Precision triple DC power supply.

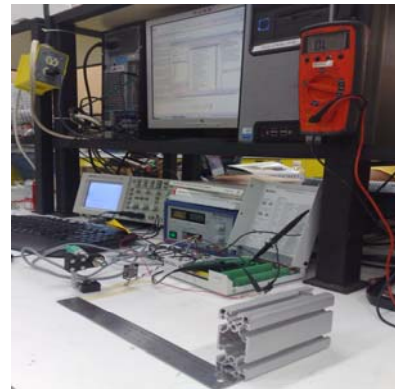


Fig. 10 Experimental Setup

We used a ruler scale to obtain the actual value of distance whereas the sensors distance from LabView provided the measured value.

### D. Obtained Data

Since the US sensor had unusable range of 0 – 50 mm and the IR sensor became saturated in the range less than 40 cm, we started taking data from 50 mm distance. Fig. 11 shows the distances measured by the US and IR sensors to given small distances between 50 to 75 mm. The accuracy percentage for the US sensor was from around 90 to 97 percent, whereas the accuracy percentage of the IR sensor was from around 92 to 95 percent. The repeatability of the IR sensor was around 97 percent which was lower than around 98 percent repeatability of the US sensor. The standard error for the US sensor was lower ranging from 1.8 to 2.4 mm than that of IR sensor ranging from 2.1 to 3.5. Therefore, we can conclude that for small distances US sensor has better resolution than IR sensor.

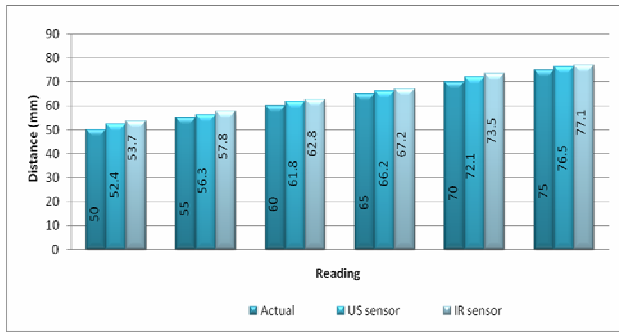


Fig. 11 Graph for small distance measurement

Next, data was acquired for longer distances between 80 to 120 mm. As can be seen in Fig. 12, the error is higher than that of the small distance analysis for both sensors.

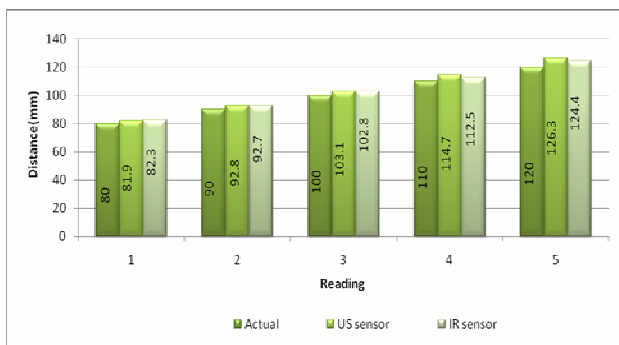


Fig. 12 Graph for longer distance measurement

In this case, the errors shown by US and IR sensors were closer ranging from 1.9 to 3.6 mm. The accuracy percentage was from around 95 to 97 percent in case of US sensor, while IR sensor provided accuracy percentage of around 97 percent. It was noted that the repeatability of both sensors was around 98 percent in second analysis.

#### F. Validation of Phong Model

To test the theory, we placed the silver metal block from the IR sensor. The angular position of the sensor was relative to the normal of the surface. Then we used (5) to find  $C_0$  and  $C_1$ . Finally, we repositioned the block and calculated the distance between the block and the sensor by using (6). Fig. 13 compares these calculated and measured distances between 7 cm and 20 cm. Above 20 cm, the infrared readings were too small, yielding inaccurate results. We followed the same procedure in case of other flat surfaces, including white plastic and unfinished wood. When the sensor was in the distances less than 10 cm, the calculated distances were more than the measured distances. Within the distances less than 10 cm, the greatest error was 0.91 cm in case of unfinished wood placed in 7 cm distance from the sensor. On the other hand, all of the calculated distances between 10 cm and 14 cm were more accurate. The greatest error in this range was 0.8 cm.

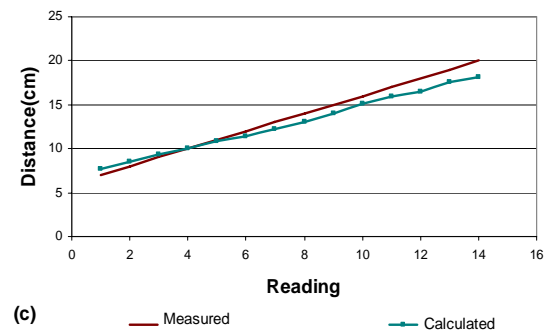
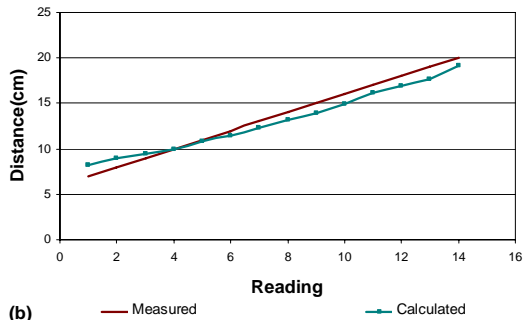
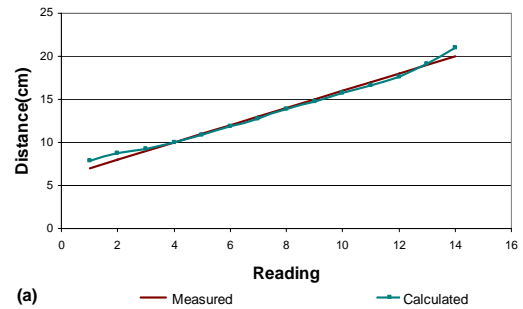


Fig. 13 Comparison of Calculated vs. Measured distance with (a) a Silver Metal Block, (b) White Plastic surface, and (c) Unfinished Wood surface

Here we positioned the obstacles manually in known distances. However, in unknown environments, the distances to obstacles must come from other sensors to determine the parameters of the Phong Model. In this experiment, we tested the US sensor which provided good accuracy and repeatability. The information on distance from the US sensor can be fed to (6) to determine the parameters  $C_0$  and  $C_1$  for the Phong Model.

#### G. Sources of Error in Distance Estimates

Equation (6) can be used to obtain an estimate of the distance from the IR sensor reading, the angle of incidence, and the reflectance properties of the obstacle. Uncertainty in any of these values will produce uncertainty in the distance estimate. Fig. 14 shows the change in US sensor readings due to angular deviation of the object surface but in the same distances. Noise in the measurement is another source of error.

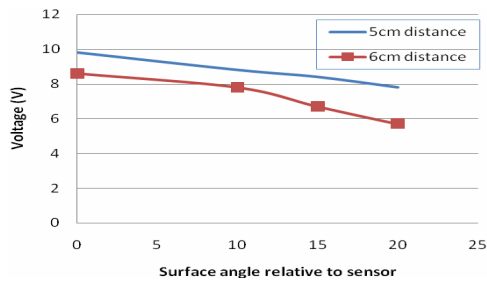


Fig. 14 Change in sensor readings due to change in angle

In the infrared sensor, phototransistors absorb infrared rays emitted from an object raise the temperature because of its continuous use. Fig. 15 shows the effect of temperature on phototransistors collector current available from manufacturer's data sheet.

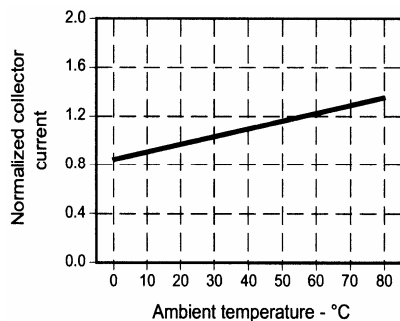


Fig. 15 Collector current vs. Temperature plot

#### V. CONCLUSION AND RECOMMENDATIONS

In this project, we focused on the ability of the sensors to detect the range of objects of flat surfaces and of different materials. The experiments indicate that the low cost US and IR sensors are able to give reliable distance measurement. The results obtained show satisfactory agreement between the Phong Illumination model and the real data obtained in the validation tests.

It has been shown that US sensor has slightly higher resolution than that of the IR sensor, especially for small distance measurement within their usable ranges. Differences between the measured distances and actual distances indicate necessary re-calibration. More care should be taken when placing the objects from the sensors during acquiring data since the small change in angle could show very different distance than the actual one. The amplitude from the US sensor is dependent on the distance and orientation of the obstacle relative to the sensor, where small orientation of the reflecting surface does not have much effect on the IR sensor amplitude. However, the amplitude from the IR sensor is dependent on the reflectivity of the obstacle, where surface color and smoothness does not have much effect on the output signal from the US sensor.

For the simplification of the calculation for Phong model, we take  $\alpha = 0$ . Therefore, a great care is taken in acquiring data so that the direction of the IR signal corresponds to the surface normal. We assumed  $C_2 = 0$  and  $n = 1$  for simplicity. Since we used flat surfaces in this experiment, we achieved

good results with these assumptions. However, for objects of non-uniform appearance we need multiple sensors besides taking these parameters into consideration.

Future works can be done on the fusion of the information supplied by the US and IR sensors that can be utilized for mobile robot navigation in unknown environment. In real environment, the obstacles could have surfaces at different angles. Moreover, when the sensor becomes very near to the obstacles, it begins to saturate. These can be mitigated by using multiple sensors and meshing the information by each sensor.

#### ACKNOWLEDGMENT

The author expresses his sincere gratitude to Professor Michael D. Naish of the department of Mechanical and Materials Engineering at the University of Western Ontario, for his valuable advice and guidance throughout the project. Thanks are due to Professor Shaun P. Salisbury for his constructive suggestions and Dave Lunn for his continuous support to complete the project successfully.

#### REFERENCES

- [1] P.M Novotny, N.J. Ferrier, "Using infrared sensor and the Phong illumination model to measure distances," International Conference on Robotics and Automation, Detroit, MI, vol. 2, April 1999, pp. 1644-1649.
- [2] G. Benet, F. Blanes, J.E. Simo, P. Perez, "Using infrared sensors for distance measurement in mobile robots," Journal of Robotics and Autonomous Systems, vol. 10, 2002, pp. 255-266.
- [3] A. Sabatini, V. Genovese, E. Guglielmelli, A. Mantuano, G. Ratti, and P. Dario, "A low-cost, composite sensor array combining ultrasonic and infrared proximity sensors," International Conference on Intelligent Robots and Systems, Pittsburgh, Pennsylvania, vol. 3, August 1995, pp. 120-126.
- [4] V. Colla, A.M. Sabatini, "A composite proximity sensor for target location and color estimation," IMEKO Sixth International Symposium on Measurement and Control in Robotics, Brussels, 1996, pp. 134-139.
- [5] L. Korba, S. Elgazzar, T. Welch, "Active infrared sensors for mobile robots," IEEE Transactions on Instrumentation and Measurement, vol. 2(43), 1994, pp. 283-287.
- [6] A.M. Sabatini, V. Genovese, E. Guglielmelli, "A low-cost, composite sensor array combining ultrasonic and infrared proximity sensors, IEEE/RSJ International Conference on Intelligent Robots and Systems (IROS), Pittsburgh, PA, vol. 3, 1995, pp. 120-126.
- [7] H.R. Everett, Sensors for Mobile Robots, AK Peters, Ltd., Wellesley, MA, 1995.
- [8] A.M. Flynn, "Combining sonar and infrared sensors for mobile robot navigation," The International Journal of Robotics Research, vol. 7(6), 1988, pp. 5-14.
- [9] G. Benet, J. Albaladejo, A. Rodas, P.J. Gil, "An intelligent ultrasonic sensor for ranging in an industrial distributed control system," IFAC Symposium on Intelligent Components and Instruments for Control Applications, Malaga, Spain, May 1992, pp. 299-303.
- [10] B. T. Phong., "Illumination for computer generated pictures," Communications of the ACM, vol. 18(6), June 1975, pp. 311-317.



**Tarek Mohammad** received Bachelor of Science degree in Mechanical Engineering from Chittagong University of Engineering & Technology, Chittagong, Bangladesh in 2007.

He is currently pursuing Master of Engineering Science in Mechanical Engineering at the University of Western Ontario, ON, Canada. He is also working as teaching assistant and research assistant under the Department of Mechanical and Materials Engineering at the University of Western Ontario, ON, Canada.

Mr. Mohammad is a student member of American Society of Mechanical Engineers (ASME) and Bangladesh Society of Mechanical Engineers (BSME).